Scientific Research Publishing

Open Journal of Geology, 2024, 14, 963-987
https://www.scirp.org/journal/ojg
ISSN Online: 2161-7589
ISSN Print: 2161-7570

Mineral Chemistry and Geochemistry as Proxy for Petrogenetic Evaluation of Charnockites: Evidences from Marandahalli, Salem Block of Southern India

Sunki Amarendhar[1*], Valluri Sai Krishna Priya[2], Malintee Vittal[2], Madabhhoshi Srinivas[2]

[1]Department of Geology, University College of Science Saifabad, Osmania University, Hyderabad, India
[2]Department of Geology, Osmania University, Hyderabad, India
Email: *amarendhar.s@gmail.com

How to cite this paper: Amarendhar, S., Priya, V.S.K., Vittal, M. and Srinivas, M. (2024) Mineral Chemistry and Geochemistry as Proxy for Petrogenetic Evaluation of Charnockites: Evidences from Marandahalli, Salem Block of Southern India. *Open Journal of Geology*, **14**, 963-987.
https://doi.org/10.4236/ojg.2024.1411043

Received: October 25, 2024
Accepted: November 24, 2024
Published: November 27, 2024

Abstract

The charnockites of Marandahalli, Dharmapuri District, Tamil Nadu India, form a part of the southern granulitic terrain in the Salem Block (SB). The charnockites are medium to coarse grained, inequigranular, with porphyroblastic and granophyric textures. They are composed of plagioclase feldspars (49 - 66 vol.%), K-feldspar (1 - 5 vol.%) and quartz (21 - 34 vol.%). The mafic minerals include pyroxene (2 - 7 vol.%) and biotite (1 - 12 vol.%). The accessory minerals include magnetite and apatite. Orthopyroxene compositions (MgO 16 - 22 wt.%) fall within the hypersthene series ($En_{55.03}Fs_{43.57}Wo_{1.4}$) and yield peak metamorphic temperatures of 800˚C - 1000˚C. Biotites show K_2O, MgO, FeO, TiO_2, and Al_2O_3 concentrations consistent with magmatic formation, and Ti-in-biotite thermometry suggests temperatures of ~740˚C - 800˚C. Plagioclase compositions (An_{26-33}) plot in the oligoclase field, while K-feldspar (Or_{93-99}) plots in the orthoclase/microcline field. A ternary feldspar geothermometer indicates a retrograde temperature of <700˚C for the rocks. The rocks are originated from the Mg rich amphibolite source and garnet free. The rocks are calc-alkaline with high SiO_2 (65 - 68 wt.%), $Na_2O > K_2O$, high CaO (3 - 5 wt.%), MgO (2.5 - 4 wt.%) and Fe_2O_3 (2 - 6 wt.%). The concentration of V, Rb and Ni, and LREE-rich and HREE-depleted patterns of the rocks indicate low degree of partial melting.

Keywords

Charnockite, Salem Block, Fractional Crystallization, Amphibolite, Marandahalli, Peninsular Gneissic Complex (PGC)

1. Introduction

The earliest identification of a rock containing hypersthene as charnockite [1] paved the way for recognizing genetically related metamorphic rocks like adakites, charnockites, enderbites, and orthopyroxene-quartz syenites collectively as the "charnockite suite" [2]. The charnockites of southern India (**Figure 1(a)**) in the form of crustal blocks of the Southern Granulite Terrain (SGT) are distributed extensively around Coorg, Salem, Biligirirangan Hills, Nilgiri, Madras, Madurai, Trivandrum, and Nagercoil and have been studied in detail [3]-[18]. The charnockitic suite of rocks effectively preserves the record of deep crustal processes and is known to mark the regions of high-pressure and high-temperature metamorphic regimes [8] [10] and is known to occur in various tectonic settings. The charnockites of southern granulite terrain in the Precambrian terranes are related to convergent margin and post-collisional extension settings during Mesoarchean to Paleoproterozoic periods [16] [19]-[25].

Charnockites have been classified into two types [4] [26]: 1) magmatic type, which comprises orthopyroxenes crystallised straight from charnockitic magma, and 2) metamorphic type, formed under low-H_2O fluid activity conditions, which give rise to the progress of dehydration reactions such as the breakdown of hornblende or biotite to develop orthopyroxene. In southern India, amphibolite-facies gneiss frequently substitutes amphibole-biotite gneiss which is typically found in highly foliated rocks/lithological units. Charnockitic rocks are also designated as orthopyroxene-bearing granites [27]-[30]. It is evident that the production of protolith of charnockites can result from the partial melting of a melt-depleted granulite source or dehydrating and partial melting of a mantle-derived underplated magma similar to that of a continental flood basalt [31] [32]. While the ferroan and transitional group of charnockites were most likely generated in extensional and continent-continent collisional tectonic settings respectively; the magnesian group charnockites are developed in magmatic arcs [26] [33] [34]. This study focuses on the mineral chemistry and geochemical characteristics of the Marandahalli charnockites to investigate their emplacement processes and tectonic setting.

2. Geology of the Study Area

The area around Marandahalli (**Figure 1(b)**) forms a part of the Krishnagiri-Kollegal terrain of the Salem Block and it is dominated by huge charnockitic massifs. These rocks often occur in elevated terrain and are bordered by granitic orthogneisses and paragneisses that have undergone amphibolite to granulite grade metamorphism [8] [35]. The Salem Block's charnockitization and metamorphism took place at around 2.50 Ga [35].

The study area is situated west of Dharmapuri Suture Rift Zone (DSRZ) [36] which is in close to the Paleoproterozoic nepheline-syenite of Pikkili and ultramafic alkaline carbonatite rock Complex of Hogenakkal. The Marandahalli charnockite contains enclaves of meta-basic rocks, granite, and pegmatites and is

traversed by dolerite. The charnockites are fresh, medium- to coarse-grained, grey in colour and exhibit gneissosity. The transformation of tonalitic gneisses to charnockite is evident from the diffuse boundaries of charnockite running gneissic foliation and banding, thereby suggesting that the charnockitic imprint on the early migmatitic fabric. The incipient charnockitization of coarse migmatitic gneisses (tonalitic gneisses) is seen at its contact with pink granite and along pegmatite veins.

Plagioclase, orthopyroxene clots, K-feldspar, quartz and biotite occur within the charnockite. These charnockitic rocks exhibit minor foliation in NNE-SSW foliation trend with easterly dips ranging from 50˚ to 70˚. Based on Sr, Nd and Pb isotope studies the tonalitic gneisses and charnockites of Krishnagiri (which are 45 km NE of the present area) were assigned a 2.5 Ga age, and the time interval between the emplacement of tonalitic precursors and granulite facies metamorphism was few tens of million years [37]. Given the similarity between the Marandahalli rocks and Krishnagiri area, it is reasonable to presume a similar age to the former.

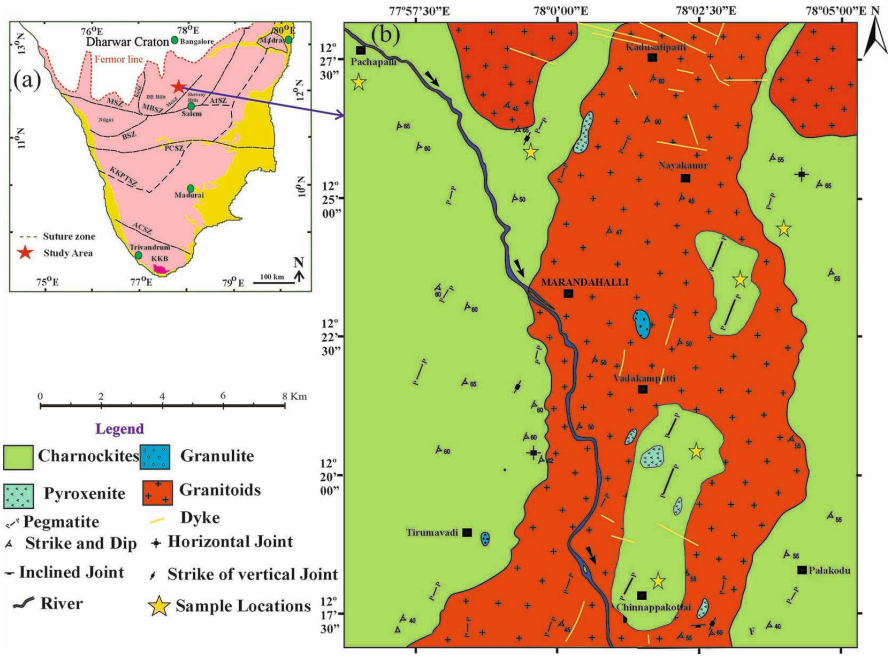

Figure 1. (a) Major shear zones of the southern India. Fermor Line: divide line between Dharwar craton and Southern Granulite Terrane (SGT) [35] [38] [39]. Major shear zones include: Moyar Shear Zone (MSZ), Bhavani Shear Zone (BSZ), Mettur Shear Zone (MeSZ), Attur Shear Zone (AtSZ), Kollegala Shear Zone (KoSZ), Palghat-Cauvery Shear Zone (PCSZ), Karur-Kambam-Painavu-Trichur Shear Zone (KKPTSZ), and Achankovil Shear Zone (AcSZ). The red colour star marks the location for this study. (b) Generalized geological map of the Marandahalli (present study).

3. Materials and Analytical Techniques

Detailed geological mapping in and around Marandahalli area was carried out to discover new locations and to collect field data as well as representative rock

samples. The laboratory studies include the preparation of polished thin sections and their detailed petrological studies to identify the mineral assemblages, textures and mineral reactions. The polished thin sections were prepared by CSIR-National Geophysical Research Institute, Hyderabad and petrography was done by the Department of Geology, University College of Science, Saifabad, Osmania University, Hyderabad. Mineralogical studies based on Electron Probe Micro Analysis was done from GSI, Hyderabad, India. Determination of major element, trace element and REE geochemistry of representative samples were carried out in the CSIR-National Geophysical Research Institute, Hyderabad. For petrographic studies, representative charnockites samples of ~6 kg weight 40 samples were collected from each location. Unaltered chip samples are collected for the preparation of thin sections. CSIR-National Geophysical Research Institute, Hyderabad was provided facilities for the preparation of representative chip samples of charnockites for thin section analysis.

The rock slices were polished on one side by using a different mess of carborundum powder (80, 200 and 400 mesh) and mounted with Araldite on a glass plate. Care was taken to remove the air bubbles by heating on a hot plate followed by pressing it from the top at an angle. Then the other side was polished using various abrasives and finally, the polishing was done using fine abrasive materials. Each type of rock was examined in terms of petrography, mineral assemblages, textural relationships, photomicrographs and modal analyses were documented.

Thin sections of selected samples were used for microprobe analysis in the present study. These thin sections (~30 μm) thick were very well polished and coated with carbon to maintain uniform electrical conductivity as well as to avoid charge built up at the spot of analysis. Each carbon coated thin section was fixed in the sample holder and silver nitrate paints were applied at the edge to connect the coated thin section and the sample holder for measuring the sample current. The areas of interest were marked, and photomicrographs were taken before each thin section was introduced into EPMA for analysis. Each area of interest was brought into the field of view and the different silicate and opaque minerals were bombarded by an electron beam for estimating their major element compositions. This was carried out at GSI, Hyderabad on EPMA (Cameca, Model: SX-100), adopting a non-destructive micron beam analytical method. The source of the beam is a Tungsten filament producing the electron beam. The beam diameter is 1 - 3 μm, under an accelerating voltage of 15 kV, beam current of 15 nA and a vacuum condition of 10 - 6 Torr.

The charnockite samples were squashed and pulverized using an agate mill and a 200-mesh pulverizer. Philips Magi PRO model (PW 2440) wavelength dispersive X-ray fluorescence spectrometer combined with an automatic sample changer (PW 2540) at CSIR-National Geophysical Research Institute, Hyderabad was used to determine the major element concentrations using pressed pellets [40] and samples were not analysed for loss on ignition (LOI). Following the closed digestion method, the materials were dissolved for trace element and RE element

analysis with the aid of Perkin Elmer Scitex ELAN DRC II ICP-MS available at the same institute. 50 mg of representative sample powders were dissolved in Saville containers containing 10 ml acid mixture of 7:3 hydrofluoric acid (HF)- nitric acid (HNO_3) combination and maintained 150˚C for 48 hours. After digestion, 2 - 3 drops of perchloric acid ($HClO_4$) were mixed, and the whole blend was evaporated to complete dryness. 20 ml of freshly prepared (1:1) HNO_3 and Milli Q H_2O was added and heated at 80˚C for 10-15 minutes on a hot plate. After getting a transparent solution, 5 ml of Rh (1ppm concentration) was added as an internal standard and the solution was adjusted to a volume of 250 ml using Milli-Q deionized water. It was then carefully stored in high-density polyethylene (HDPE) bottles, each with a capacity of 60 ml. From each HDPE bottle, 5 ml of the sample solution was extracted and further diluted to 50 ml, achieving a dilution level of 50,000 times. Analysis of trace elements, including Rare Earth Elements (REEs), was conducted using High Resolution 28ctively Coupled Plasma Mass Spectrometry (HR-ICP-MS).

4. Discussion and Results

4.1. Petrography

Under the microscope, the charnockites exhibit medium to coarse-grained granoblastic texture. The grains have well-defined boundaries and occasionally large grains of orthopyroxene are noticed in some sections (**Figure 2**). Plagioclase and quartz are the dominant minerals with appreciable amounts of pyroxene. Biotite, magnetite and apatite occur as accessory minerals and the rocks are garnet-free.

Plagioclase occurs are fresh with albite, pericline and occasional carlsbad twinning. It shows characteristic antiperthitic texture with coarse blebs of K-feldspar elongated parallel to the twin lamellae and rarely cutting across them. It contains inclusions of quartz and apatite and shows an alter to sericite. Anhedral grains of quartz show undulate extinction. Orthopyroxene (hypersthene) occurs as sub-idiomorphic grains showing characteristic pleochroism from light green to pale yellow. It encloses hornblende and biotite suggesting a reaction relationship between them (**Figures 2(a)-(f)**).

This relation and the orthopyroxene grains closely mimicking the shape and mineral fabric orientation of the biotite and hornblende indicate the prograde transformation of hornblende and biotite to orthopyroxene. However, some pyroxene grains show hornblende rims around them in which case it appears that hornblende is later than pyroxene suggesting local retrograde metamorphism. The retrogression might probably have resulted due to local fluctuation in physical conditions or during shearing. The modal compositions of the rocks of Marandahalli fall in the charnockite (tonalitic) field of the QAP diagram [4] [41]-[43] (**Figure 3(a)**).

4.2. Mineral Chemistry

Mineral chemistry plots (EPMA) of various minerals, such as orthopyroxene,

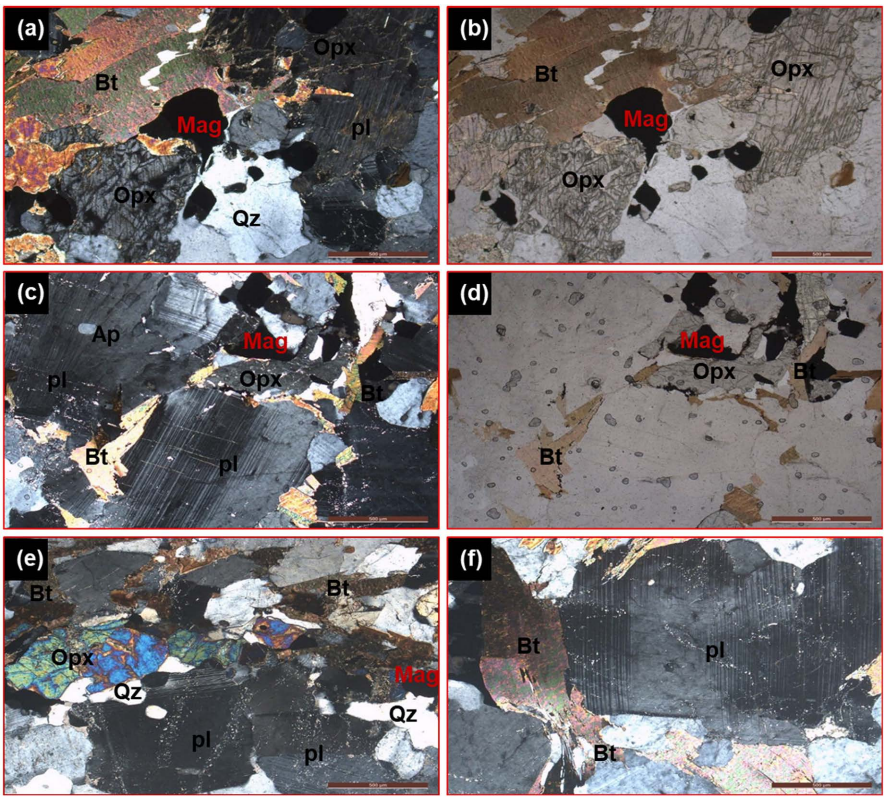

Figure 2. Photomicrographs of the charnockites from Marandahalli, Dharmapuri District, Tamil Nadu. (a) & (b) Phenocryst of pyroxene associated with plagioclase, biotite, quartz and magnetite. (c)-(e) Photomicrograph showing the pyroxene(hypersthene) phenocrysts associated with biotite, magnetite, apatite and plagioclase minerals. (f) Photomicrograph showing the twinned plagioclase and biotite.

biotite, K-feldspar and plagioclase and their respective SGT charnockitic areas like Marandahalli, Madurai, Coorg and Nagercoil (**Table 1**). The orthopyroxene of charnockites of Maranadahalli has MgO ranging from 16 - 22 wt.% (**Table 2**), and falls in the hypersthene composition of ($En_{55.03}$ $Fs_{43.57}$ $Wo_{1.4}$) enstatite-ferrosilite solid solution series [44] (**Figure 3(b)**). It exhibits varying Mg# (0.50 to 0.71), and plot in the igneous pyroxenes field in the XMg Vs Al diagram (**Figure 3(c)**) similar to the pyroxenes of charnockites from Coorg [45], on the contrary the charnockites of the Madurai Block [46] and the Nagercoil [47] that plot in metamorphic pyroxene field (**Figure 3(c)**).

The biotites have abundant K_2O 8 - 10 wt.%, MgO 10 - 16 wt.%, FeO 13 - 20 wt.%, TiO_2 4 - 6 wt.%, and Al_2O_3 13 - 15 wt.% (**Table 2**) respectively. The Fe/(Fe + Mg) ratio in biotite is 0.38 - 0.50 with an average of 0.58 and the Si vs. Fe/Fe + Mg diagram is plotted in the biotite field (**Figure 3(d)**) [48]. These biotites appear to be formed in the last phase of magmatism. The analyzed biotites (**Table 2**) plot in the primary biotite field in the $10TiO_2$-(FeO + MnO)-MgO diagram (**Figure 4(a)**) [49]. For composition, the biotites from the charnockites of Madurai [46], Nagercoil [47] and Coorg [45] are also shown in **Figure 3(d)** and **Figure 4(a)**.

Plagioclase exhibit consisting of anorthite (An_{26-33}) content along with the

plagioclase from charnockits of Madurai [46] and Nagercoil [47] also get plotted in the anorthite field (**Figure 4(b)** and **Table 3**). However, the plagioclase from charnockites of Coorg [45] gets plotted in the albite to andesine fields (**Figure 3(f)**). K-feldspar being in the composition of Marandahalli varying in range Or_{93-99} and plotted in the orthoclase/microcline field (**Table 3**; **Figure 4(b)**) and other charnockite plutons are also getting in similar fields.

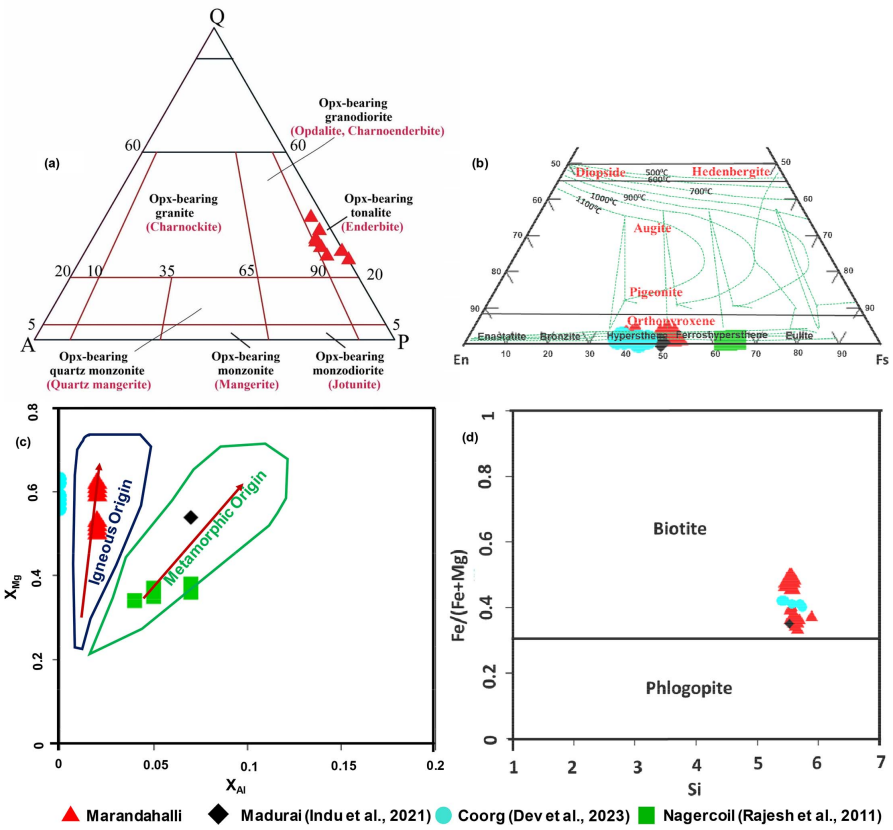

Figure 3. (a) QAP diagram showing the plots of Marandahalli charnockites [4] [41]-[43]. (b) Compositions of pyroxene are shown in the diagram of wollastonite, enstatite, and ferrosilite [44]. Pyroxene thermometry at 5 kbar, the polythermal orthopyroxene-augite-pigeonite relations are also depicted in the plotting [50]. (c) XMg = (Mg/(Fe + Mg)) vs XAl = (Al/2) diagram illustrating the chemistry of orthopyroxenes. According to [47], the arrow in the plot depicts the compositional trend of orthopyroxene in the igneous rock. (d) Composition of mica in the charnockites of Marandahalli in Si vs Fe/(Fe + Mg) end member classification diagrams for mica [48].

4.3. Geochemistry

The whole rock composition of Marandahalli charnockites (major, trace and RE elements) are provided in **Table 4** & **Table 5**) and are marked by a high SiO_2 concentration (~65 - 69 wt.%) and a reasonably high Al_2O_3 (~12 - 15 wt.%). They exhibit the metaluminous nature in terms of the Alumina Saturation Index (ASI) (**Figure 5(a)**), along with those from Coorg, Madurai and Nagercoil. However, some of the Nagercoil charnockites [47] displaying a slightly peraluminous nature [52]. The Modified Alkali-Lime Indices (MALI) [53] of Marandahalli indicates a

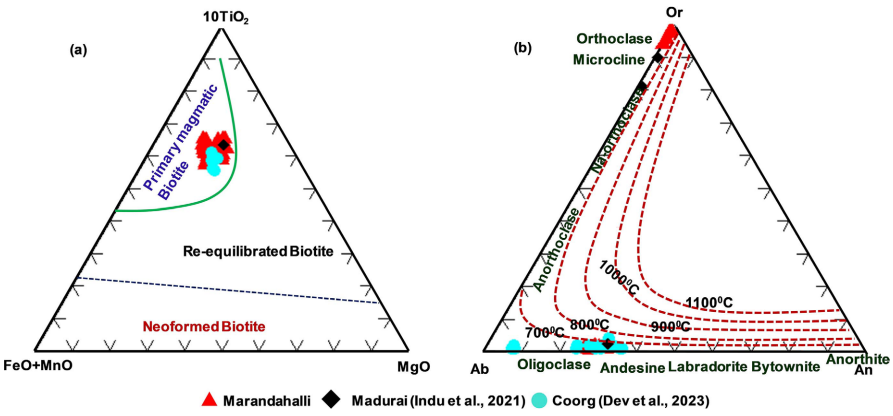

Figure 4. (a) Ternary diagram showing domains of primary magmatic, re-equilibrated and Neo-formed biotites [49]. (b) An-Ab-Or system [51] showing the plots of the feldspar compositions in charnockite. Note the restricted range of compositions of K-feldspar and plagioclase, for explanation see the text.

Table 1. Mineral chemistry plots of various minerals and their respective SGT charnockitic areas.

	Area	Pyroxene	Mica	K-feldspar	Plagioclase
▲	Marandahalli (Present Study)	Opx	Biotite	Microcline	Oligoclase-Andesine
◆	Madurai [46]	Opx	Biotite	Microcline	Oligoclase-Andesine
●	Coorg [45]	Opx	Biotite	Microcline	Albite-Andesine
■	Nagercoil [47]	Opx	-	-	-

Table 2. Electron Probe Micro Analysis (EPMA) of pyroxene and biotite mineral chemistry from charnockites of Marandahalli and adjoining charnockite plutons.

Area	1 (16)		2 (1)	3 (6)		4 (14)		5 (43)		6 (5)		7 (1)
Mineral in Wt.%	Orthopyroxene							Biotite				
No. oxygen	6			6		6		11		11		11
	Range	Average		Range	Average	Range	Average	Range	Average	Range	Average	
SiO_2	49.81 - 53.19	51.67	49.63	47.92 - 48.70	48.14	49.92 - 52.96	52.15	34.64 - 38.08	36.56	35.64 - 37.44	36.64	37.22
TiO_2	0.02 - 0.11	0.06	0.14	0.02 - 0.07	0.05	0.70 - 3.65	1.32	4.12 - 5.55	4.81	3.56 - 5.01	4.04	5.01
Al_2O_3	0.71 - 0.94	0.83	3.22	1.51 - 2.94	2.25	0.01 - 0.11	0.05	13.22 - 14.83	14.04	14.42 - 17.34	15.57	14.84
FeO	23.11 - 30.35	26.46	27.02	36.20 - 37.60	36.78	22.70 - 27.07	25.07	13.16 - 19.67	16.53	13.84 - 16.93	15.88	13.84
MnO	0.41 - 0.97	0.68	1.21	0.05 - 0.25	0.16	0.23 - 1.38	0.8	0 - 0.22	0.08	0.01 - 0.13	0.08	0.13
MgO	16.59 - 21.79	19.25	17.64	11.02 - 12.15	11.67	19.38 - 21.82	20.34	10.61 - 15.30	12.62	12.24 - 14.68	13	14.68
CaO	0.49 - 1.25	0.68	0.15	0.27 - 0.41	0.33	0.13 - 0.74	0.47	0 - 0.47	0.06	0 - 0.02	0.01	0.02
Na_2O	0.01 - 0.06	0.02	0.01	0.02 - 0.40	0.24	0 - 0.06	0.02	0 - 0.17	0.06	0.02 - 0.15	0.09	0.02
K_2O	nd	nd	nd	nd	nd	nd	nd	8 - 9.82	9.3	nd	nd	nd
Si	1.96 - 1.99	1.97	1.92	1.92 - 1.95	1.94	1.91 - 1.99	1.97	5.44 - 5.89	5.59	5.4 - 5.57	5.58	5.53
Al	0.03 - 0.04	0.04	0.1	0.07 - 0.14	0.1	0	0	2.39 - 2.65	2.53	2.53 - 3.19	2.81	2.6

Continued

Ti	0	0	0	0	0	0	0	0.47-0.65	0.55	0.42-0.57	0.5	0.56
Fe(ii)	0.68 - 0.97	0.85	0.87	1.12 - 1.21	1.23	0.71 - 0.86	0.79	1.71 - 2.51	2.12	1.71 - 2.11	2.04	1.72
Mn	0.01 - 0.03	0.02	0.04	0 - 0.02	0.01	0.01 - 0.04	0.03	0 - 0.03	0.01	0 - 0.3	0.01	0.02
Mg	1.22 - 0.96	1.09	1.02	0.66 - 0.72	0.7	1.10 - 1.22	1.14	2.46 - 3.40	2.87	2.74 - 3.24	2.9	3.25
Ca	0.02 - 0.05	0.03	0.01	0.01 - 0.02	0.01	0.01 - 0.03	0.02	0 - 0.08	0.01	0 - 0.03	0	0
Na	0	0	0	0.01 - 0.03	0.02	nd	nd	0 - 0.05	0.02	0.01 - 0.05	0.03	0
K	nd	nd	nd	nd	nd	nd	nd	1.58 - 1.94	1.81	1.81 - 1.9	1.88	1.86
Wo	1 - 2.60	1.4	0.32	0.59 - 0.91	0.72	1.0 - 2.0	0.93	-	-	-	-	-
En	48.59 - 60.62	55.03	52.54	34.19 - 37.19	35.86	56 - 62	58.5	-	-	-	-	-
Fs	38.29 - 49.90	43.57	47.13	62.22 - 64.91	63.42	36 - 44	40.57	-	-	-	-	-
XMg	0.50 - 0.71	0.42	0.39	0.38 - 0.34	0.24	0.56 - 0.63	0.45	0.52 - 0.67	5.58	0.58 - 0.60	0.59	0.51
XFe	0.38 - 0.50	0.58	0.61	0.62 - 0.66	0.76	0.37 - 0.44	0.55	0.33 - 0.50	0.42	0.40 - 0.42	0.41	0.49
XAl	0 - 0.02	0.02	0.05	0.04 - 0.07	0.05	-	-	-	-	-	-	-
FeO + MnO	-	-	-	-	-	-	-	13.30 - 19.69	16.61	15.35 - 17.15	15.96	13.97
10TiO_2	-	-	-	-	-	-	-	41.18 - 55.51	48.08	35.60 - 44.50	40.36	50.1

1, 5 [Present work work]; 2, 7 Madurai—Indu *et al.* 2021; 3 Nagarcoil—Rajesh *et al.* 2011; 4, 6 Coorg—Dev *et al.* 2023; nd = not determined; (*) Number of mineral grains.

Table 3. Electron Probe Micro Analysis (EPMA) of feldspars mineral chemistry from charnockites of Marandahalli and adjoining charnockite plutons.

Area	**1 (21)**		**2 (27)**		**3 (1)**	**4 (6)**		**5 (2)**	
Mineral in wt.%	**Plagioclase**							**K-feldspar**	
No. oxygen	**08**			**08**		**08**		**08**	
	Range	**Average**	**Range**	**Average**		**Range**	**Average**	**Range**	**Average**
SiO_2	60.05 - 63.42	61.27	59.53 - 68.4	63.17	60.49	62.20 - 63.91	63.11	63.85 - 64.90	64.375
TiO_2	0 - 0.07	0.01	0 - 0.05	0.01	0.04	0	0	0 - 0.01	0.005
Al_2O_3	22.61 - 24.46	23.52	19.74 - 25.60	23.28	24.81	17.25 - 18.34	17.8	18.69 - 18.77	18.73
FeO	0 - 0.19	0.05	0 - 0.09	0.03	0.09	0 - 0.06	0.02	0.01 - 0.03	0.02
MnO	0 - 0.05	0.01	0 - 0.05	0.01	0.02	0 - 0.02	0	0 - 0.02	0.01
MgO	0 - 0.02	0	0 - 0.03	0.01	nd	0 - 0.03	0.01	nd	nd
CaO	5.47 - 6.84	6.15	1.47 - 7.53	4.69	6.47	0	0	0.12 - 0.24	0.18
Na_2O	6.95 - 8.60	7.91	7.16 - 11.31	9.01	7.56	0.19 - 0.63	0.39	1.01 - 1.91	1.46
K_2O	0.12 - 0.46	0.26	0.14 - 0.71	0.27	0.43	14.80 - 1626	15.6	13.4 - 14.88	14.14
Si	10.83 - 11.19	10.98	10.61 - 11.76	11.74	10.78	11.93 - 12.12	12.02	11.92 - 11.96	11.94
Ti	0 - 0.01	0	0 - 0.01	0	0.01	0	0	0	0
Al	4.77 - 5.12	4.97	4.18 - 5.38	4.84	5.21	3.85 - 4.09	3.99	4.08 - 4.11	4.095

Continued

Fe(ii)	0 - 0.03	0.01	0 - 0.01	0	0.01	0 - 0.01	0	0	0
Ca	1.04 - 1.31	1.18	0.28 - 1.44	0.89	1.24	0	0	0.02 - 0.05	0.035
Na	2.38 - 2.98	2.75	2.47 - 3.88	3.08	2.61	0.07 - 0.24	0.14	0.37 - 0.68	0.525
K	0.03 - 0.11	0.06	0.03 - 0.16	0.06	0.1	3.63 - 3.93	3.79	3.15 - 3.54	3.345
An	25.90 - 32.79	29.62	7.0 - 36.0	21.99	31.31	0	0	0.8 - 1.04	0.92
Ab	65.05 - 73.31	68.91	63 - 92	76.49	66.21	1.80 - 6.11	3.66	12.62 - 14.26	13.44
Or	0.71 - 2.71	1.47	1.0 - 2.0	1.52	2.48	93.89 - 98.20	96.34	83.87 - 87.41	85.64

1, 4 [Present work work]; 2 Coorg—Dev *et al.* 2023; 3, 5 Madurai—Indu *et al.* 2021; nd = not determined; (*) Number of mineral grains.

distinct calcic signature, while the Nagercoil charnockites [47] show calcic to calc-alkalic nature (**Figure 5(b)**). Even based on their Fe number [53], the Marandahalli charnockites along with the charnockite of other plutons [45]-[47] [54] depicts in magnesian rich nature (**Figure 5(c)**). In the TAS diagram, the charnockite samples show granodiorite to granite composition and display a distinctive sub-alkali trend (**Figure 5(d)**). The result in the samples plotting in high Sr + Ba granite field (**Figure 6**) on the Sr-Rb-Ba ternary diagram [55] [56] is resulted of the low Rb and high Sr and Ba of the charnockites from the study area. Furthermore, the high Sr + Ba content of these rocks may be a result of mafic and felsic melt mixing and mingling from the lower crust and enriched mantle [57].

The charnockites of Marandahalli are derived from (meta-igneous) amphibolite source indicated by the low ratios of $(Na_2O + K_2O)/(FeO^t + MgO + TiO_2)$ and $(Na_2O + K_2O + FeO^t + MgO + TiO_2)$ [58] (**Figure 7(a)**), which is also reflected in the $Al_2O_3/(FeO + MgO + TiO_2)$ vs. $(Al_2O_3 + FeO + MgO + TiO_2)$ plot (**Figure 7(b)**) and when the charnockites from the Marandahalli along with charnockite rocks of other areas of SGT. The Mg# vs. SiO_2 binary plot of charnockites (**Figure 7(c)**) suggests the origin of charnockites be related to the melting of pre-existing continental crust with dehydration within the mantle. Even, the $^{+ve}$Eu anomalies strengthen the observation that these rocks may have been formed by the re-melting of (metamorphic rocks) TTGs, supra-crustals or amphibolites. The lithological variations in the continental crust (ultramafic to felsic) to much diversified charnockites could be a consequence of re-melting of crust and possibly the interaction with mantle may be promoted by the diversity in charnockites aided by mantle dynamics and plate tectonics [59]. Against this scenario, given the limitations, it is thus surmised that the protoliths of Marandahalli formations have been initiated by the melting of amphibolite, followed by intra-crustal re-melting of protoliths of Marandahalli within the plagioclase stability and removal of potassic melt. Thus, the primary source of protolith is mantle melt, with a little amount of crustal contribution.

Mafic granulites are found in the charnockites as enclaves, and even the geochemical data is suggestive of an amphibolitic source (**Figure 7(d)**) for the

charnockites parent magma. The usual Archean TTG nature of these rocks is revealed together with high Sr/Y ratios (**Figure 7(d)**), perhaps TTGs underwent charnockite transformation. However, the Kollaimalai and Pachaimalai [54], the Nagercoil charnockite [47] and Coorg charnockites [45] exhibit a spread over the Archaen TTG to arc magma fields. The overall petrological and geochemical similarity of the Marandahalli charnockites and the Archean TTG suites suggests that these rocks were derived from amphibolite. The Marandahalli charnockites exhibit lower Sr/Y values in contrast with melts derived from garnet-bearing ecologitic sources (that contain high Sr/Y and low Y values) due to the partitioning of Y into residual garnet [60] and are broadly similar to melts yielded by garnet free amphibolitic sources. It can be stated that enrichment of amphibole and plagioclase in the residue, along with an LILE-enrichment is noticed in the Marandahalli charnockites.

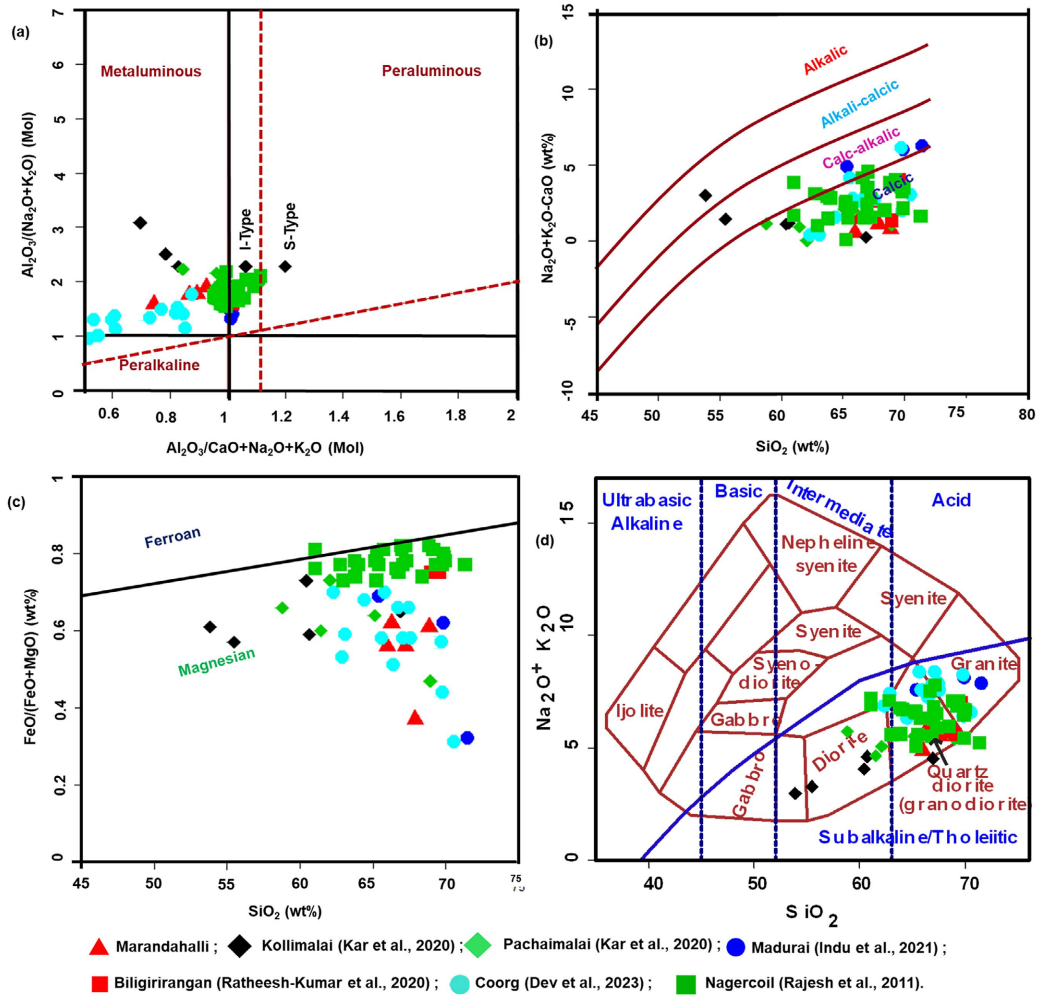

Figure 5. Marandahalli charnockites exhibit a distinct geochemical signature. (a) The Alumina Saturation Index diagram from [52] illustrates the charnockite are metaluminous character. (b) Alkali-lime index diagram shows calcic to calc-alkalic nature [53]. (c) The magnesian character is demonstrated in $FeO^{tot}/(FeO^{tot} + MgO)$ vs. SiO_2 discrimination [53]. (d) The charnockite of Marandahalli is classified as granodiorite in plots of SiO_2 vs. $Na_2O + K_2O$ (TAS) [61].

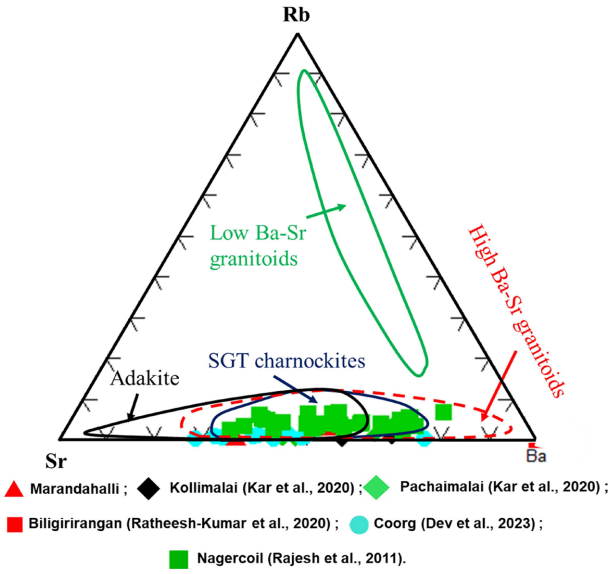

Figure 6. The Sr-Rb-Ba ternary plot for the charnockites in the Marandahalli area. The sources for the fields for high- and Low-Ba-Sr granitoids [55] [56].

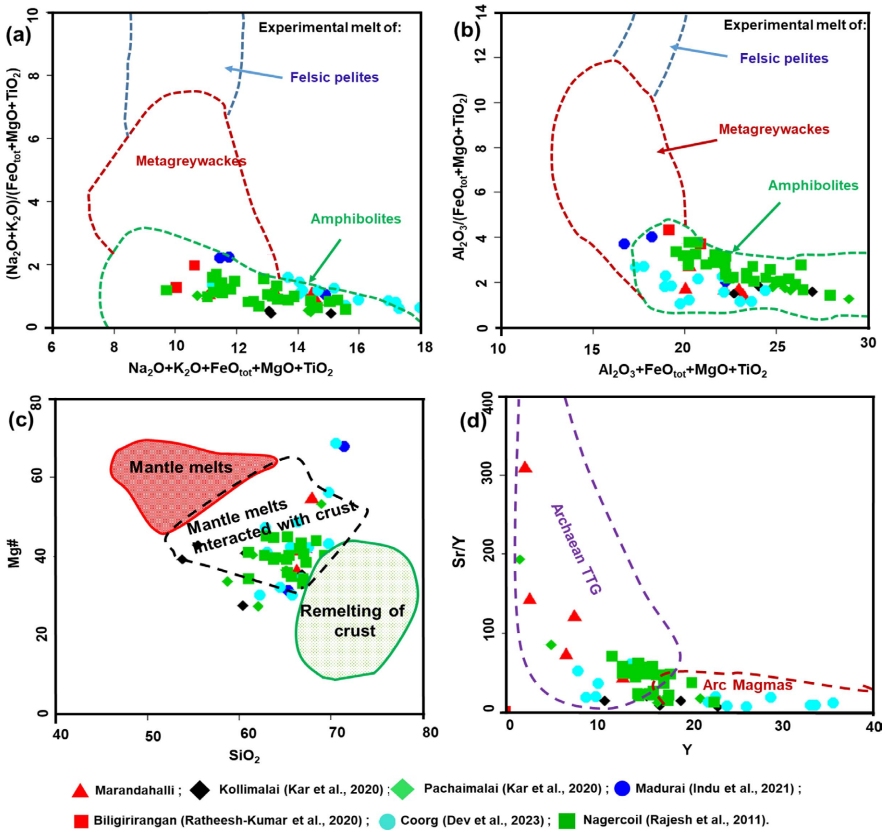

Figure 7. (a) (b) Binary plots relating the compositions of experimental melts generated by the partial melting of felsic pelites, metagreywackes, and amphibolite/metabasalt-metatonalites with compositional fields of the sources for the development of charnockites [57]. The values are all expressed in wt%. (c) Mg number (Mg#) vs. SiO_2 (wt%) plot with in the mantle melts interacting with crustal source source [59]. (d) Sr/Y vs. Y (ppm) plot; fields depicting Archean source [62].

Table 4. Major Oxide (wt%) analyses of Marandahalli charnockites.

	Major oxides in wt.%							
Area	**1**	**2**	**3**	**4**	**5**	**SY-3***	Range	Average
SiO_2	67.22	65.98	66.28	68.86	67.89	59.67	65.98 - 68.86	67.25
Al_2O_3	13.77	13.45	14.25	12.56	14.75	11.75	12.56 - 14.75	13.76
$Fe_2O_3^t$	4.73	5.58	5.56	4.37	2.08	6.48	2.08 - 5.58	4.46
MnO	0.03	0.02	0.01	0.05	0.02	0.31	0.01 - 0.05	0.03
MgO	3.38	3.89	3.12	2.51	3.17	2.65	2.51 - 3.89	3.21
CaO	3.22	4.31	4.34	4.95	4.48	8.24	3.22 - 4.95	4.26
Na_2O	3.28	4.30	3.19	3.02	3.16	4.13	3.02 - 4.30	3.39
K_2O	2.43	0.56	2.58	2.71	2.41	4.22	0.56 - 2.71	2.14
TiO_2	0.30	0.27	0.01	0.60	0.27	0.15	0.01 - 0.60	0.29
P_2O_5	0.18	0.10	0.03	0.16	0.12	0.53	0.03 - 0.18	0.12
Total	98.54	98.46	99.37	99.79	98.35	98.13	98.35 - 99.79	98.92
Ratios								
XFe	0.56	0.56	0.62	0.61	0.37		0.37 - 0.62	0.54
XMg	41.68	41.08	35.94	36.48	54.42		35.94 - 54.42	41.92
$Na_2O + K_2O + Fe_2O_3^t + MgO + TiO_2$	14.12	14.60	14.46	13.21	11.09		11.09 - 14.60	13.50
$(Na_2O + K_2O)/(Fe_2O_3^t + MgO + TiO_2)$	1.13	0.83	1.03	1.14	1.01		0.83 - 1.14	1.03
$Al_2O_3 + Fe_2O_3^t + MgO + TiO_2$	22.18	23.19	22.94	20.04	20.27		20.04 - 23.19	21.72
$Al_2O_3/(Fe_2O_3^t + MgO + TiO_2)$	1.64	1.38	1.64	1.68	2.67		1.38 - 2.67	1.80
K_2O/Al_2O_3	0.18	0.04	0.18	0.22	0.16		0.04 - 0.22	0.16
Na_2O/Al_2O_3	0.24	0.32	0.22	0.24	0.21		0.21 - 0.32	0.25
$(Na_2O + K_2O)$-CaO	2.49	0.55	1.43	0.78	1.09		0.55 - 2.49	1.27
$Na_2O + K_2O$	5.71	4.86	5.77	5.73	5.57		4.86 - 5.77	5.53

*Standard analysis.

Table 5. Trace and REE (ppm) analyses of Marandahalli charnockites.

	Trace elements in ppm								
Area	**1**	**2**	**3**	**4**	**5**	**SY-2***	**SY-2***	**Range**	**Average**
Sc	6.2	1.82	7.69	11.62	2.36	7	7.28	1.82 - 11.62	5.94
V	50.57	24.51	90.28	69.55	28.09	50	50.92	24.51 - 90.28	52.6
Cr	38.01	39.77	123.96	47.88	117.16	9.5	9.51	38.01 - 123.96	73.35
Co	7.17	6.25	14.01	13.57	6.46	8.6	8.76	6.25 - 14.01	9.49
Ni	8.2	7.77	18.74	10.73	10.88	9.9	10.07	7.77 - 18.74	11.27
Cu	5.31	6.1	14.62	4.6	8.21	5.2	5.27	4.60 - 14.62	7.77
Zn	55.26	38.12	240.14	51.35	168.21	248	250.99	38.12 - 240.14	110.62
Ga	16.06	14.7	17.93	17.68	16.01	29	29.32	14.70 - 17.93	16.48

Continued

Rb	84	1.6	27.72	52.08	29.09	217	217.44	1.60 - 84.00	38.9
Sr	899	662.62	470.8	528.36	375.25	271	271.56	375.25 - 899	587.2
Y	7.52	2.15	6.6	12.78	2.65	128	128.11	2.15 - 12.78	6.34
Zr	59.18	43.78	51.69	64.86	59.16	280	280.91	43.78 - 64.86	55.74
Nb	5.21	2	4.28	6.54	2.93	29	29.31	2 - 6.54	4.19
Cs	0.15	0.05	0.09	0.24	0.14	2.4	2.45	0.05 - 0.24	0.13
Ba	2010.17	388.17	624.61	700.29	411.03	460	468.11	411.03 - 2010.17	826.85
Hf	1.45	1.11	1.33	1.78	1.47	7.7	7.69	1.11 - 1.78	1.43
Ta	1.27	0.18	0.41	0.65	0.16	2.01	2	0.16 - 1.27	0.53
Pb	31.85	21.69	28.8	28.31	26.15	85	85.83	21.69 - 31.85	27.36
Th	1.44	0.59	0.88	4.18	2.06	379	388.44	0.59 - 4.18	1.83
U	0.21	0.18	0.2	0.31	0.43	284	288.76	0.18 - 0.43	0.27
Sr/Y	119.48	308.62	71.31	41.33	141.49	7	7.28	41.33 - 308.62	136.45
La/Nb	7.15	7.09	9.03	5.27	8.23	50	50.92	5.27 - 9.03	7.35
Th/Nb	0.28	0.3	0.21	0.64	0.7	9.5	9.51	0.21 - 0.70	0.42
U/Nb	0.04	0.09	0.05	0.05	0.15	8.6	8.76	0.04 - 0.15	0.07
Rare Earth Elements in ppm									
La	37.27	14.2	38.62	34.5	24.09	75	76.388	14.20 - 37.27	29.74
Ce	61.06	22.07	65.72	64.95	38.9	175	177.159	22.07 - 65.72	50.54
Pr	6.17	2.07	5.95	6.83	3.22	18.8	18.991	2.07 - 6.83	4.85
Nd	22.38	7.17	20.9	26.55	10.38	73	73.416	7.17 - 26.55	17.48
Sm	3.52	0.96	3.27	4.91	1.4	16.1	16.118	0.96 - 4.91	2.81
Eu	1.79	0.82	1.29	1.28	0.73	2.42	2.416	0.73 - 1.79	1.18
Gd	2.63	0.81	2.54	3.95	1.11	17	16.962	0.81 - 3.95	2.21
Tb	0.25	0.07	0.23	0.41	0.09	2.5	2.498	0.07 - 0.41	0.21
Dy	1.3	0.37	1.21	2.24	0.47	18	17.94	0.37 - 2.24	1.12
Ho	0.22	0.06	0.21	0.37	0.08	3.8	3.818	0.06 - 0.37	0.19
Er	0.59	0.16	0.56	0.99	0.21	12.4	12.421	0.16 - 0.99	0.5
Tm	0.08	0.02	0.08	0.14	0.03	2.1	2.105	0.02 - 0.14	0.07
Yb	0.54	0.17	0.53	0.95	0.21	17	16.845	0.17 - 0.95	0.48
Lu	0.08	0.03	0.08	0.14	0.03	2.7	2.706	0.03 - 0.14	0.07

*Standard analysis.

4.4. Pressure and Temperature

The Ca-Fe-Mg-pyroxene phase relations at 500˚C - 1200˚C and 1 bar to 15 kbar, for estimating geo-thermometry of Marandahalli charnockites by utilizing ortho-pyroxene assemblage [50]. The resulting curve in the pyroxene quadrilateral (**Figure 3(b)**) yields temperatures ranging from 1000˚C - 1100˚C and pointing to the peak metamorphism or the crystallisation stage of pyroxene. The crystallization temperatures of charnockites can be deduced from binary plots like SiO_2 vs. TiO_2 and SiO_2 vs. P_2O_5. The charnockites plots between the isotherms of 700 ˚C - 800˚C (isotherms of Coorg charnockites are marginally higher) on SiO_2 vs. TiO_2 plot

(**Figure 8(a)**) and temperature between 750˚C - 850˚C in the SiO_2 vs. P_2O_5 plot (**Figure 8(b)**). **Table 4** demonstrates a lower TiO_2 content in the charnockites of Marandahalli mostly confined in an average 0.30 wt.% (ranges: 0.01 - 0.6 wt.%). **Figure 8(a)** and b show the Fe-Ti [63] and apatite saturation temperatures [64] for the Marandahalli charnockites stand at 7.5 kbar. Charnockitic rocks and the consistent decrease in temperature with increasing SiO_2 contents could be a result of fractionating charnockite intrusion [65].

Ilmenite is present in the samples under study and biotite falls within the requisite compositional ranges for Ti (0.47 - 0.65) and XMg (0.50 - 0.67), the Ti in biotite thermometer is used in this particular study. The Ti in biotite thermometer and pressure values have an estimated uncertainty of (P = 400 - 600 MPa) used in their calibration [66]. The metamorphic temperatures obtained by Ti thermometry for all charnockite samples are ~740˚C - 800˚C (**Figure 8(c)**). The ternary feldspar geo-thermometer diagram is using plagioclase composition on An-Ab-Or [67] less than 700˚C is shown for the rocks under study show (**Figure 4(b)**), that may correspond to a late retrograde temperature of magnesian charnockite.

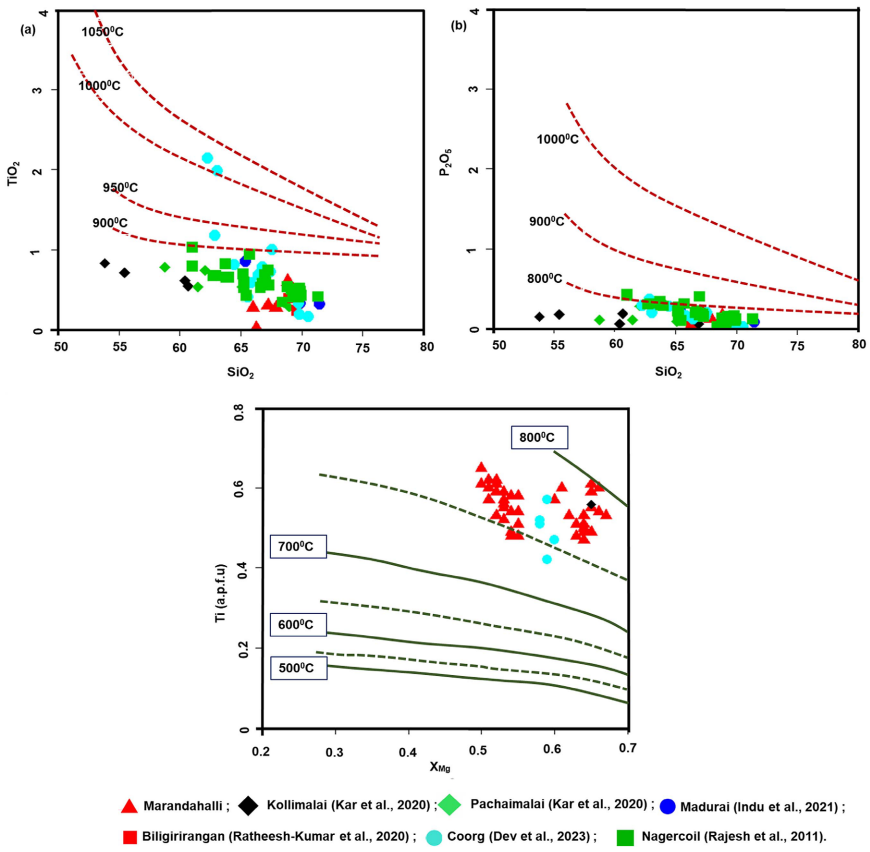

Figure 8. (a) TiO_2 versus SiO_2 and (b) P_2O_5 versus SiO_2 plots of the Marandahalli charnockite samples. The isotherms in (a) show Fe-Ti oxide saturation temperatures at 7.5 kbar [63], while those in (b) illustrate apatite saturation temperatures at 7.5 kbar [64]. (c) Biotite composition for the Marandahalli charnockite with temperature contours [66]. The dashed curves represent the intermediate 50˚C interval isotherms. Symbols in the diagram show the Ti (a.p.f.u.) vs. Mg/(Mg + Fe) of biotites from different samples in this study.

4.5. Tectonic Setting

The systematics of trace elements are used to understand the tectonic evolution of the charnockite rocks of Marandahalli, which display a significantly higher La/Nb ratio, and as made evident in the Nb versus La/Nb variation diagram (**Figure 9(a)**) [68] characterize the charnockites to be subduction-related magma plots. Even, La/Nb vs. Th/Nb (**Figure 9(b)**) and La/Nb vs. U/Nb (**Figure 9(c)**) demonstrate the charnockites have subduction-related magma source, and that these rocks exhibit substantially higher LILE/HFSE elemental ratios (**Figure 9**) [68]. The tectonic descrimnation diagrams *i.e.* Zr vs. Nb/Zr diagram (**Figure 9(d)**) [69], also hint a subduction field setting. Charnockites are plotted in the volcanic arc granite plot (VAG) [70]. Immobile elemental systematics also support the subduction-derived magmatism in the volcanic arc granites (VAG) field in the tectonic discrimination diagram (**Figure 10(a)**).

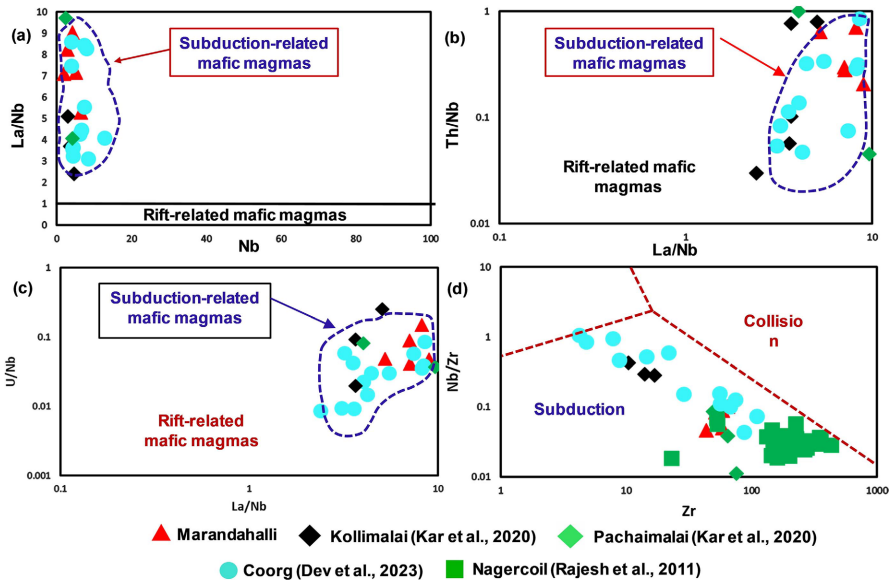

Figure 9. (a) The charnockite Nb against La/Nb variation diagram clearly indicates a higher La/Nb ratio, which is the typical sign of subduction-related magmas. (b) La/Nb vs. Th/Nb. (c) The La/Nb vs. U/Nb variation diagram indicates a subduction-related magma source for the charncokites. Note that the charnockite samples are found in the mafic magma zone associated with subduction [68]. (d) The tectonic setting diagram shows the relationship between Nb/Zr and Zr. Similar to the majority of the charnockites in southern India, all of the charnockites are restricted to the subduction field [69].

The Cr (38 - 124 ppm) and Ni (7 - 19 ppm) contents in charnockites are extremely varied but relate to SiO_2. The plots like Ni and V vs. Rb and Ni vs. Ba plots can be effectively used to illustrate the corresponding importance of fractional crystallisation (FC) and partial melting (PM). While, partial melting produces sub-horizontal patterns in differentiated magmas, fractional crystallisation produces almost vertical trends [71] [72]. It is observed that the PM process dominants the other processes, Ni vs. Rb (**Figure 10(b)**) as reflected by preventing one

from favouring either mechanism. However, on V vs. Rb (**Figure 10(c)**) and Ni vs. Ba plots (**Figure 10(d)**), the Marandahalli follow flat coherent trends suggesting the role of partial melting in their petrogenitic evolution.

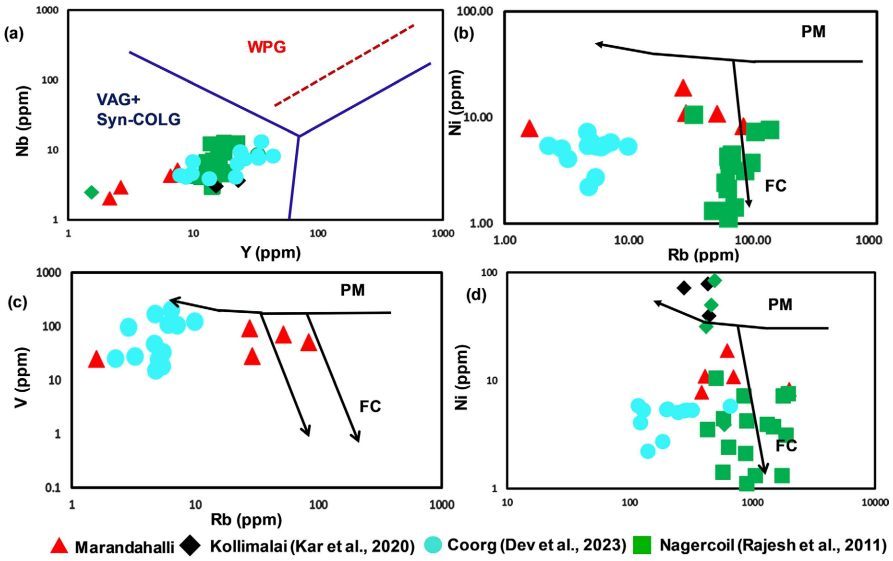

Figure 10. (a) The charnockites are restricted to the volcanic arc granite (VAG) in discriminating diagram for granite [70]. Partial melting patterns were seen for the Marandahalli charnockite samples on the log-log distribution plots of compatible vs. incompatible trace elements [71] [72]. Three examples are (b) Ni vs. Rb, (c) V vs. Rb, and (d) Ni vs. Ba. The evolutionary patterns via partial melting and fractional crystallisation are shown, respectively, by the classifications PM (sub-horizontal arrows) and FC (sub-vertical arrows).

Charnockites from the study area marked by the enrichment of large ion lithophile elements (LILE). The multi-element spider diagrams [73] (**Figure 11(a)**) display prominent troughs of Nb, P, and Ti indicating mineral phases like magnetite, apatite and sphene are retained in the subduction source, and peaks at Ba and Pb indicate that they go into melt phase. The positive anomalies Th and Sr indicate they have entered into feldspars. The normalised REE chondrite patterns display [74] enrichment of the LREE and depletion of HREE in these rocks indicate a low degree of partial melting in the source, a feature that is common to the charnockites/granites that formed in the continental arc setting; and the subtle positive Eu anomaly is due to the incorporation of plagioclase (fractionation/separation) in the rock (**Figure 11(b)**).

Though the charnockites have an igneous parentage [37] [75], however, [76] advocate a sedimentary parentage to these rocks. They suggested a sedimentary (psammite and pelite-dominated greywacke-type) genesis for the charnockites using major element discrimination (ASI > 1.1; negative values of discriminant factor (DF) and oxygen isotope data [77]. However, they may also form by the melting of biotite-bearing metaluminous felsic rocks [78] or even by water-excess melting of mafic rocks [79]. Further, igneous enclaves present within Marandahalli charnockite strongly hints that more mafic magmas and/or other igneous

sources may have been involved in the origin of igneous types of magma [80] [81] (Figure 11(c) & Figure 11(d)).

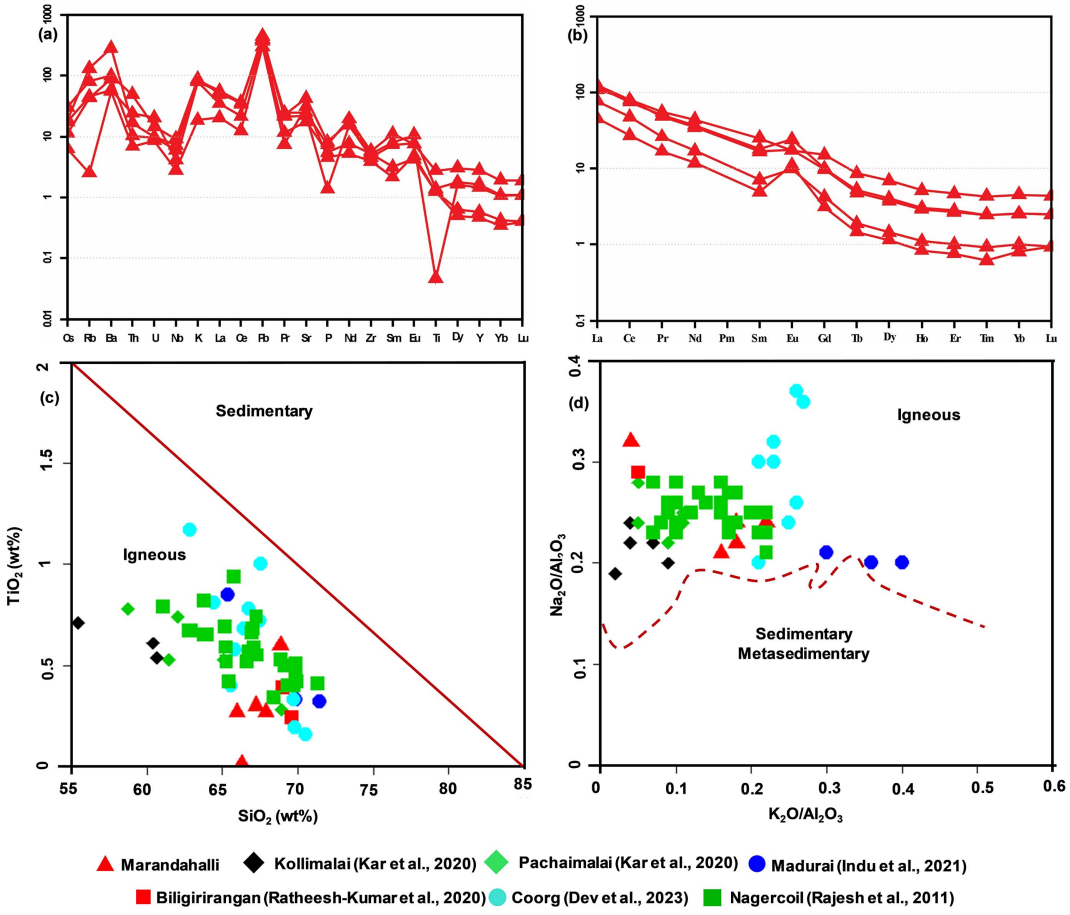

Figure 11. (a) Multi-element diagrams of primitive mantle normalisation and, (b) chondrite normalised REE patterns for the Marandahalli charnockites. Primitive and chondrite mantle-normalization factors were obtained from [73] and [74]. (c) & (d) Plots illustrating the igneous affinity of charnockites from Marandahalli. The igneous-sedimentary separation lines in the TiO_2-SiO_2 and Na_2O/Al_2O_3-K_2O/Al_2O_3 classification diagrams [80] [81].

5. Conclusions

- The Marandahalli charnockites are silica oversaturated and metaluminous, with calcic signatures and a tonalitic composition.
- The orthopyroxene in the rocks is of igneous nature. Mg pyroxene phases suggest formation temperatures in the range of 700˚C - 850˚C, while feldspar formed at temperatures less than 700˚C.
- The apatite saturation temperatures for the Marandahalli charnockites are at 7.5 kbar.
- A convergent setting is considered more favourable for the development of these arc-related rocks. The rocks are meta-igneous, characterized by an amphibolite garnet-free nature, indicating a metamorphic modification of igneous rocks.

- The protolithic source rocks are inferred to be Archean TTG suites (Tonalite –Trondhjemite-Granodiorite).
- The evolution of the Marandahalli charnockites involved the mixing and mingling of mafic and felsic melts derived from an enriched mantle and lower crust.

Acknowledgements

The authors extend sincere thanks to the Head, Department of Geology for the support and encouragement. The authors also wish to thank the Directors, National Geophysical Research Institute and Geological Survey of India, Hyderabad for providing the facilities for carrying out analytical work. The authors thank the reviewers for their suggestions and comments on how to make the paper better. The authors also acknowledge present article forms a part of the Major Research Project sanctioned to M. Srinivas by UGC, New Delhi for providing fellowship (F. No. 41-1023/201(SR).

Author Statement

S. Amarendhar: Carried out fieldwork, geochemical analysis, data interpretation and write-up of the initial version. V. Sai Krishna Priya: Draft preparation. M. Vittal: Carried out fieldwork and data interpretation. M. Srinivas: Contributed to the initial version and overall supervision of the work.

Conflicts of Interest

The authors declare no conflicts of interest regarding the publication of this paper.

References

[1] Holland, T.H. (1900) The Charnockite Series: A Group of Archæan Hypersthenic Rocks in Peninsular India (Vol. 28, No. 2). Office of the Geological Survey.

[2] Subramaniam, A.P. (1960) Petrology of the Charnockite Suite of Rocks from the Type Area Around St. Thomas Mount and Pallavaram Near Madras City, India, Internal. *International Geological Congress* 21st., Copenhagen, 15-25 August 1960, 394-403.

[3] Clark, C., Collins, A.S., Santosh, M., Taylor, R. and Wade, B.P. (2009) The *P-T-t* Architecture of a Gondwanan Suture: REE, U-Pb and Ti-in-Zircon Thermometric Constraints from the Palghat Cauvery Shear System, South India. *Precambrian Research*, **174**, 129-144. https://doi.org/10.1016/j.precamres.2009.07.003

[4] Rajesh, H.M. and Santosh, M. (2012) Charnockites and Charnockites. *Geoscience Frontiers*, **3**, 737-744. https://doi.org/10.1016/j.gsf.2012.07.001

[5] Samuel, V.O., Santosh, M., Liu, S., Wang, W. and Sajeev, K. (2014) Neoarchean Continental Growth through Arc Magmatism in the Nilgiri Block, Southern India. *Precambrian Research*, **245**, 146-173. https://doi.org/10.1016/j.precamres.2014.02.002

[6] Li, S., Santosh, M., Ganguly, S., Thanooja, P.V., Sajeev, K., Pahari, A., *et al.* (2018) Neoarchean Microblock Amalgamation in Southern India: Evidence from the Nallamalai Suture Zone. *Precambrian Research*, **314**, 1-27. https://doi.org/10.1016/j.precamres.2018.05.017

[7] Santosh, M. (2020) The Southern Granulite Terrane: A Synopsis. *Episodes*, **43**, 109-

123. https://doi.org/10.18814/epiiugs/2020/020006

[8] Janardhan, A.S., Newton, R.C. and Hansen, E.C. (1982) The Transformation of Amphibolite Facies Gneiss to Charnockite in Southern Karnataka and Northern Tamil Nadu, India. *Contributions to Mineralogy and Petrology*, **79**, 130-149. https://doi.org/10.1007/bf01132883

[9] Santosh, M. and Yoshida, M. (1992) A Petrologic and Fluid Inclusion Study of Charnockites from the Lützow-Holm Bay Region, East Antarctica: Evidence for Fluid-Rich Metamorphism in the Lower Crust. *Lithos*, **29**, 107-126. https://doi.org/10.1016/0024-4937(92)90036-x

[10] Ronald Frost, B. (2000) Origin of the Charnockites of the Louis Lake Batholith, Wind River Range, Wyoming. *Journal of Petrology*, **41**, 1759-1776. https://doi.org/10.1093/petrology/41.12.1759

[11] Santosh, M., Xiao, W.J., Tsunogae, T., Chetty, T.R.K. and Yellappa, T. (2012) The Neoproterozoic Subduction Complex in Southern India: SIMS Zircon U-Pb Ages and Implications for Gondwana Assembly. *Precambrian Research*, **192**, 190-208. https://doi.org/10.1016/j.precamres.2011.10.025

[12] Tomson, J.K., Bhaskar Rao, Y.J., Vijaya Kumar, T. and Choudhary, A.K. (2013) Geochemistry and Neodymium Model Ages of Precambrian Charnockites, Southern Granulite Terrain, India: Constraints on Terrain Assembly. *Precambrian Research*, **227**, 295-315. https://doi.org/10.1016/j.precamres.2012.06.014

[13] Collins, A.S., Clark, C. and Plavsa, D. (2014) Peninsular India in Gondwana: The Tectonothermal Evolution of the Southern Granulite Terrain and Its Gondwanan Counterparts. *Gondwana Research*, **25**, 190-203. https://doi.org/10.1016/j.gr.2013.01.002

[14] Yang, Q., Santosh, M., Rajesh, H.M. and Tsunogae, T. (2014) Late Paleoproterozoic Charnockite Suite within Post-Collisional Setting from the North China Craton: Petrology, Geochemistry, Zircon U–pb Geochronology and Lu-Hf Isotopes. *Lithos*, **208**, 34-52. https://doi.org/10.1016/j.lithos.2014.08.020

[15] Vishwakarma, N. and Thomas, H. (2015) Petrographic and Geochemical Characteristics of Charnockite from Asind, District-Bhilwara, Rajasthan: Implications for Its Origin. *Journal of Applied Geochemistry*, **17**, 10-21.

[16] Liu, P.H., Liu, F.L., Cai, J., Yang, H., Wang, F., Liu, C.H., Liu, J.H. and Shi, J.R. (2016) Metamorphic PT Conditions and Timing of the Wuchuan Garnet Mafic Granulite from the Yinshan Block, North China Craton: Insight from Phase Equilibria and Zircon U-Pb Dating. *Acta Petrologica Sinica*, **32**, 1949-1979.

[17] Gao, P. and Santosh, M. (2020) Mesoarchean Accretionary Mélange and Tectonic Erosion in the Archean Dharwar Craton, Southern India: Plate Tectonics in the Early Earth. *Gondwana Research*, **85**, 291-305. https://doi.org/10.1016/j.gr.2020.05.004

[18] Yang, C., Santosh, M., Tsunogae, T., Shaji, E., Gao, P. and Kwon, S. (2021) Global Type Area Charnockites in Southern India Revisited: Implications for Earth's Oldest Supercontinent. *Gondwana Research*, **94**, 106-132. https://doi.org/10.1016/j.gr.2021.03.003

[19] Zhai, M., Guo, J. and Liu, W. (2005) Neoarchean to Paleoproterozoic Continental Evolution and Tectonic History of the North China Craton: A Review. *Journal of Asian Earth Sciences*, **24**, 547-561. https://doi.org/10.1016/j.jseaes.2004.01.018

[20] Endo, T., Tsunogae, T., Santosh, M. and Shaji, E. (2012) Phase Equilibrium Modeling of Incipient Charnockite Formation in NCKFMASHTO and Mnnckfmashto Systems: A Case Study from Rajapalaiyam, Madurai Block, Southern India. *Geoscience Frontiers*, **3**, 801-811. https://doi.org/10.1016/j.gsf.2012.05.005

[21] Shaji, E., Santosh, M., He, X., Fan, H., Dev, S.G.D., Yang, K., *et al.* (2014) Convergent Margin Processes during Archean–proterozoic Transition in Southern India: Geochemistry and Zircon U–pb Geochronology of Gold-Bearing Amphibolites, Associated Metagabbros, and TTG Gneisses from Nilambur. *Precambrian Research*, **250**, 68-96. https://doi.org/10.1016/j.precamres.2014.05.021

[22] Yellappa, T., Venkatasivappa, V., Koizumi, T., Chetty, T.R.K., Santosh, M. and Tsunogae, T. (2014) The Mafic–ultramafic Complex of Aniyapuram, Cauvery Suture Zone, Southern India: Petrological and Geochemical Constraints for Neoarchean Suprasubduction Zone Tectonics. *Journal of Asian Earth Sciences*, **95**, 81-98. https://doi.org/10.1016/j.jseaes.2014.04.023

[23] Sarkar, T. and Schenk, V. (2014) Two-stage Granulite Formation in a Proterozoic Magmatic Arc (ongole Domain of the Eastern Ghats Belt, India): Part 1. Petrology and Pressure–temperature Evolution. *Precambrian Research*, **255**, 485-509. https://doi.org/10.1016/j.precamres.2014.07.026

[24] Santosh, M., Yang, Q., Ram Mohan, M., Tsunogae, T., Shaji, E. and Satyanarayanan, M. (2014) Cryogenian Alkaline Magmatism in the Southern Granulite Terrane, India: Petrology, Geochemistry, Zircon U-Pb Ages and Lu-Hf Isotopes. *Lithos*, **208**, 430-445. https://doi.org/10.1016/j.lithos.2014.09.016

[25] Tang, L., Santosh, M. and Teng, X. (2015) Paleoproterozoic (ca. 2.1-2.0Ga) Arc Magmatism in the Fuping Complex: Implications for the Tectonic Evolution of the Trans-North China Orogen. *Precambrian Research*, **268**, 16-32. https://doi.org/10.1016/j.precamres.2015.07.001

[26] Frost, B.R. and Frost, C.D. (2008) On Charnockites. *Gondwana Research*, **13**, 30-44. https://doi.org/10.1016/j.gr.2007.07.006

[27] Pichamuthu, C.S. (1960) Charnockite in the Making. *Nature*, **188**, 135-136. https://doi.org/10.1038/188135a0

[28] Santosh, M., Harris, N.B.W., Jackson, D.H. and Mattey, D.P. (1990) Dehydration and Incipient Charnockite Formation: A Phase Equilibria and Fluid Inclusion Study from South India. *The Journal of Geology*, **98**, 915-926. https://doi.org/10.1086/629461

[29] Kumar, G.R. and Raghavan, V. (1992) The Incipient Charnockites of Transition Zone, Granulite Zone and Khondalite Zone of South India: Contrasting Mechanisms and Controlling Factors. *Journal of Geological Society of India*, **39**, 293-302.

[30] Newton, R.C. and Tsunogae, T. (2014) Incipient Charnockite: Characterization at the Type Localities. *Precambrian Research*, **253**, 38-49. https://doi.org/10.1016/j.precamres.2014.06.021

[31] Sheraton, J.W. (1982) Origin of Charnockitic Rocks of MacRobertson Land. In: Craddock, C., Ed., A*ntarctic Geoscience*, Madison University of Wisconsin Press, 489-497.

[32] Munksgaard, N.C., Thost, D.E. and Hensen, B.J. (1992) Geochemistry of Proterozoic Granulites from Northern Prince Charles Mountains, East Antarctica. *Antarctic Science*, **4**, 59-69. https://doi.org/10.1017/s0954102092000129

[33] Rajesh, H.M. (2007) The Petrogenetic Characterization of Intermediate and Silicic Charnockites in High-Grade Terrains: A Case Study from Southern India. *Contributions to Mineralogy and Petrology*, **154**, 591-606. https://doi.org/10.1007/s00410-007-0211-y

[34] Mikhalsky, E.V. and Kamenev, I.A. (2013) Recurrent Transitional Group Charnockites in the East Amery Ice Shelf Coast (East Antarctica): Petrogenesis and Implications on Tectonic Evolution. *Lithos*, **175**, 230-243.

https://doi.org/10.1016/j.lithos.2013.05.004

[35] Ghosh, J.G., de Wit, M.J. and Zartman, R.E. (2004) Age and Tectonic Evolution of Neoproterozoic Ductile Shear Zones in the Southern Granulite Terrain of India, with Implications for Gondwana Studies. *Tectonics*, **23**, TC3006. https://doi.org/10.1029/2002tc001444

[36] Gopalakrishnan, K. and Subramanian, K.S. (2007) Inherited Geochemical Characteristics of Palaeo-Domains by Alkaline Complexes and Related Rocks within Southern Granulite Terrain, India-Implications of Crustal Contamination in Their Genesis and Emplacement. *Geological Society of India*, **69**, 684-698.

[37] Peucat, J.J., Vidal, P., Bernard-Griffiths, J. and Condie, K.C. (1989) Sr, Nd, and Pb Isotopic Systematics in the Archean Low- to High-Grade Transition Zone of Southern India: Syn-Accretion vs. Post-Accretion Granulites. *The Journal of Geology*, **97**, 537-549. https://doi.org/10.1086/629333

[38] Drury, S.A., Harris, N.B.W., Holt, R.W., Reeves-Smith, G.J. and Wightman, R.T. (1984) Precambrian Tectonics and Crustal Evolution in South India. *The Journal of Geology*, **92**, 3-20. https://doi.org/10.1086/628831

[39] Santosh, M., Yokoyama, K., Biju-Sekhar, S. and Rogers, J.J.W. (2003) Multiple Tectonothermal Events in the Granulite Blocks of Southern India Revealed from EPMA Dating: Implications on the History of Supercontinents. *Gondwana Research*, **6**, 29-63. https://doi.org/10.1016/s1342-937x(05)70643-2

[40] Krishna, A.K., Murthy, N.N. and Govil, P.K. (2007) Multielement Analysis of Soils by Wavelength-Dispersive X-Ray Fluorescence Spectrometry. *Atomic Spectroscopy-Norwalk Connecticut*, **28**, 202-214.

[41] Streckeisen, A. (1974) Classification and Nomenclature of Plutonic Rocks Recommendations of the IUGS Subcommission on the Systematics of Igneous Rocks. *Geologische Rundschau*, **63**, 773-786. https://doi.org/10.1007/bf01820841

[42] Streckeisen, A. (1976) To Each Plutonic Rock Its Proper Name. *Earth-Science Reviews*, **12**, 1-33. https://doi.org/10.1016/0012-8252(76)90052-0

[43] Maitre, L.E. (1989) A Classification of Igneous Rocks and Glossary of Terms. Recommendations of the International Union of Geological Sciences Subcommission on the Systematics of Igneous Rocks. Cambridge University Press, 193.

[44] Morimoto, N. (1988) Nomenclature of Pyroxenes. *Mineralogy and Petrology*, **39**, 55-76. https://doi.org/10.1007/bf01226262

[45] Dev, S.G.D., Shaji, E., Santosh, M., Tsunogae, T. and Prasanth, R.S. (2023) Mesoarchean Charnockites from the Coorg Block, Southern India: Petrology, Geochemistry and Tectonic Implications. *Geosystems and Geoenvironment*, **2**, Article 100134. https://doi.org/10.1016/j.geogeo.2022.100134

[46] Indu, G., Shaji, E., Binojkumar, R.B., Santosh, M. and Tsunogae, T. (2021) Petrology of Charnockites from Madurai Block of Southern Granulite Terrain, South India. *Bulletin of Pure & Applied Sciences-Geology*, **40**, 25-37. https://doi.org/10.5958/2320-3234.2021.00004.4

[47] Rajesh, H.M., Santosh, M. and Yoshikura, S. (2010) The Nagercoil Charnockite: A Magnesian, Calcic to Calc-Alkalic Granitoid Dehydrated during a Granulite-Facies Metamorphic Event. *Journal of Petrology*, **52**, 375-400. https://doi.org/10.1093/petrology/egq084

[48] Rieder, M., Cavazzini, G., D'yakonov, Y.S., Frank-Kamenetskii, V.A., Gottardi, G., Guggenheim, S., *et al.* (1998) Nomenclature of the Micas. *Clays and Clay Minerals*, **46**, 586-595. https://doi.org/10.1346/ccmn.1998.0460513

[49] Nachit, H., Ibhi, A., Abia, E.H. and Ben Ohoud, M. (2005) Discrimination between Primary Magmatic Biotites, Reequilibrated Biotites and Neoformed Biotites. *Comptes Rendus. Géoscience*, **337**, 1415-1420. https://doi.org/10.1016/j.crte.2005.09.002

[50] Lindsley, D.H. (1983) Pyroxene Thermometry. *American Mineralogist*, **68**, 477-493.

[51] Smith, J.V. (1974) Intergrowths of Feldspars with Other Minerals. In: Smith, J.V., Ed., *Feldspar Minerals*, Springer, 553-647. https://doi.org/10.1007/978-3-642-65743-6_8

[52] Shand, S.J. (1943) Eruptive Rocks: Their Genesis, Composition, Classification, and Their Relation to Ore-Deposits with a Chapter on Meteorite. John Wiley & Sons.

[53] Frost, B.R., Barnes, C.G., Collins, W.J., Arculus, R.J., Ellis, D.J. and Frost, C.D. (2001) A Geochemical Classification for Granitic Rocks. *Journal of Petrology*, **42**, 2033-2048. https://doi.org/10.1093/petrology/42.11.2033

[54] Kar, R., Bhattacharya, S., Basei, M. and Chaudhary, A.K. (2020) Petrological and Geochronological Constraints on the Evolution of Charnockitic Rocks in the Massifs of Cauvery Shear Zone, Southern Granulite Terrain, India. *Journal of the Geological Society of India*, **95**, 527-537. https://doi.org/10.1007/s12594-020-1472-6

[55] Fowler, M.B. and Henney, P.J. (1996) Mixed Caledonian Appinite Magmas: Implications for Lamprophyre Fractionation and High Ba-Sr Granite Genesis. *Contributions to Mineralogy and Petrology*, **126**, 199-215. https://doi.org/10.1007/s004100050244

[56] Fowler, M.B., Henney, P.J., Darbyshire, D.P.F. and Greenwood, P.B. (2001) Petrogenesis of High Ba-Sr Granites: The Rogart Pluton, Sutherland. *Journal of the Geological Society*, **158**, 521-534. https://doi.org/10.1144/jgs.158.3.521

[57] Tarney, J. and Jones, C.E. (1994) Trace Element Geochemistry of Orogenic Igneous Rocks and Crustal Growth Models. *Journal of the Geological Society*, **151**, 855-868. https://doi.org/10.1144/gsjgs.151.5.0855

[58] Patiño Douce, A.E. (1999) What Do Experiments Tell Us about the Relative Contributions of Crust and Mantle to the Origin of Granitic Magmas? *Geological Society, London, Special Publications*, **168**, 55-75. https://doi.org/10.1144/gsl.sp.1999.168.01.05

[59] Halla, J., Whitehouse, M.J., Ahmad, T. and Bagai, Z. (2016) Archaean Granitoids: An Overview and Significance from a Tectonic Perspective. *Geological Society, London, Special Publications*, **449**, 1-18. https://doi.org/10.1144/sp449.10

[60] Martin, H. (1987) Petrogenesis of Archaean Trondhjemites, Tonalites, and Granodiorites from Eastern Finland: Major and Trace Element Geochemistry. *Journal of Petrology*, **28**, 921-953. https://doi.org/10.1093/petrology/28.5.921

[61] Cox, K.G., Bell, J.D. and Pankhurst, R.J. (1979) The Interpretation of Data for Plutonic Rocks. In: Cox, K.G., Bell, J.D. and Pankhurst, R.J., Eds., *The Interpretation of Igneous Rocks*, Springer, 308-331. https://doi.org/10.1007/978-94-017-3373-1_13

[62] Defant, M.J. and Drummond, M.S. (1990) Derivation of Some Modern Arc Magmas by Melting of Young Subducted Lithosphere. *Nature*, **347**, 662-665. https://doi.org/10.1038/347662a0

[63] Green, T.H. and Pearson, N.J. (1986) Ti-Rich Accessory Phase Saturation in Hydrous Mafic-Felsic Compositions at High P,T. *Chemical Geology*, **54**, 185-201. https://doi.org/10.1016/0009-2541(86)90136-1

[64] Harrison, T.M. and Watson, E.B. (1984) The Behavior of Apatite during Crustal Anatexis: Equilibrium and Kinetic Considerations. *Geochimica et Cosmochimica Acta*, **48**, 1467-1477. https://doi.org/10.1016/0016-7037(84)90403-4

[65] Grantham, G.H., Eglington, B.M., Thomas, R.J. and Mendonidis, P. (2001) The Nature of the Grenville-Age Charnockitic A-Type Magmatism from the Natal, Namaqua

and Maud Belts of Southern Africa and Western Dronning Maud Land, Antarctica. Memoirs of National Institute of Polar Research, 59-86.

[66] Henry, D.J. (2005) The Ti-Saturation Surface for Low-to-Medium Pressure Metapelitic Biotites: Implications for Geothermometry and Ti-Substitution Mechanisms. *American Mineralogist*, **90**, 316-328. https://doi.org/10.2138/am.2005.1498

[67] Fuhrman, M.L. and Lindsley, D.H. (1988) Ternary-Feldspar Modeling and Thermometry. *American Mineralogist*, **73**, 201-215.

[68] Kumar, K.V., Rathna, K. and Leelanandam, C. (2015) Proterozoic Subduction-Related and Continental Rift-Zone Mafic Magmas from the Eastern Ghats Belt, SE India: geo-Chemical Characteristics and Mantle Sources. *Current Science*, **108**, 184-197.

[69] Thieblemont, D. and Tegyey, M. (1994) Geochemical Discrimination of Differentiated Magmatic Rocks Attesting for the Variable Origin and Tectonic Setting of Calc-Alkaline Magmas. *Comptes Rendus de l'Académie des Sciences Série II*, **319**, 87-94.

[70] Pearce, J.A., Harris, N.B.W. and Tindle, A.G. (1984) Trace Element Discrimination Diagrams for the Tectonic Interpretation of Granitic Rocks. *Journal of Petrology*, **25**, 956-983. https://doi.org/10.1093/petrology/25.4.956

[71] Cocherie, A. (1986) Systematic Use of Trace Element Distribution Patterns in Log-Log Diagrams for Plutonic Suites. *Geochimica et Cosmochimica Acta*, **50**, 2517-2522. https://doi.org/10.1016/0016-7037(86)90034-7

[72] De Souza, Z.S., Martin, H., Peucat, J., Jardim De Sá, E.F. and Macedo, M.H.D.F. (2007) Calc-Alkaline Magmatism at the Archean-Proterozoic Transition: The Caicó Complex Basement (NE Brazil). *Journal of Petrology*, **48**, 2149-2185. https://doi.org/10.1093/petrology/egm055

[73] Sun, S.-S. and McDonough, W.F. (1989) Chemical and Isotopic Systematics of Oceanic Basalts: Implications for Mantle Composition and Processes. *Geological Society, London, Special Publications*, **42**, 313-345. https://doi.org/10.1144/gsl.sp.1989.042.01.19

[74] Boynton, W.V. (1984) Cosmochemistry of the Rare Earth Elements: Meteorite Studies. *Developments in Geochemistry*, **2**, 63-114. https://doi.org/10.1016/b978-0-444-42148-7.50008-3

[75] Condie, K.C. and Allen, P. (1984) Origin of Archaean Charnockites from Southern India. In: Kröner, A., Hanson, G.N. and Goodwin, A.M., Eds., *Archaean Geochemistry: The Origin and Evolution of the Archaean Continental Crust*, Springer, 182-203. https://doi.org/10.1007/978-3-642-70001-9_9

[76] Raith, M.M., Srikantappa, C., Buhl, D. and Koehler, H. (1999) The Nilgiri Enderbites, South India: Nature and Age Constraints on Protolith Formation, High-Grade Metamorphism and Cooling History. *Precambrian Research*, **98**, 129-150. https://doi.org/10.1016/s0301-9268(99)00045-5

[77] Shaw, D.M. (1972) The Origin of the Apsley Gneiss, Ontario. *Canadian Journal of Earth Sciences*, **9**, 18-35. https://doi.org/10.1139/e72-002

[78] Miller, C.F. (1985) Are Strongly Peraluminous Magmas Derived from Pelitic Sedimentary Sources? *The Journal of Geology*, **93**, 673-689. https://doi.org/10.1086/628995

[79] Ellis, D.J. and Thompson, A.B. (1986) Subsolidus and Partial Melting Reactions in the Quartz-Excess $CaO+MgO+Al_2O_3+SiO_2+H_2O$ System under Water-Excess and Water-Deficient Conditions to 10 kb: Some Implications for the Origin of Peraluminous Melts from Mafic Rocks. *Journal of Petrology*, **27**, 91-121.

https://doi.org/10.1093/petrology/27.1.91

[80] Mackenzie, F.T. and Garrels, R.M. (1971) Evolution of Sedimentary Rocks. Norton.

[81] Tarney, J. (1976) Geochemistry of Archaean High-Grade Gneisses, with Implications as to the Origin and Evolution of the Precambrian Crust. In: Windley, B.F. Ed., *The Early History of the Earth*, Wiley, 405-424.